Scale up of single-chamber microbial fuel cells with stainless steel 3D anode: Effect of electrode surface areas and electrode spacing

Justine Papillon, Olivier Ondel, Eric Maire

Bioresource Technology Reports

Scale up of single-chamber microbial fuel cells with stainless steel 3D anode: effect of electrode surface areas and electrode spacing.

Justine PAPILLON [a,*] Olivier ONDEL [b] Éric MAIRE [a]

a: Univ. Lyon - INSA Lyon - MATEIS, UMR CNRS 5510, F-69100 Villeurbanne, France

b: Univ. Lyon, Université Claude Bernard Lyon 1, École Centrale de Lyon, INSA Lyon, CNRS, Ampère, F-69621, Villeurbanne, France

Abstract

Single-chamber microbial fuel cells (MFCs) with air-cathodes and new anodes made of stainless steel entangled wires are developed. Increasing the cathode surface area significantly increases performances (doubling the cathode surface area increases the maximum power by +23,3 % and tripling it by +59,8 %.). By contrast, increasing the anode surface area rapidly leads to performance saturation (doubling the anode surface area increases the maximum power by +37.8 % but tripling it by only +39.3 %.). In addition, decreasing the electrode spacing from 6 cm to 4 cm improves the maximum power by +21.3 % and from 4 cm to 2 cm by +27.9 %. This results permit to optimally dimension the architecture of the MFC in order to maximize energy production while minimizing the amount of materials used to minimize costs. This in turn is likely to enable the development of effective solutions for energy harvesting.

Keyword

Microbial fuel cells ; Stainless steel anode ; Cathode surface area ; Anode surface area ; Electrode spacing.

Graphical abstract

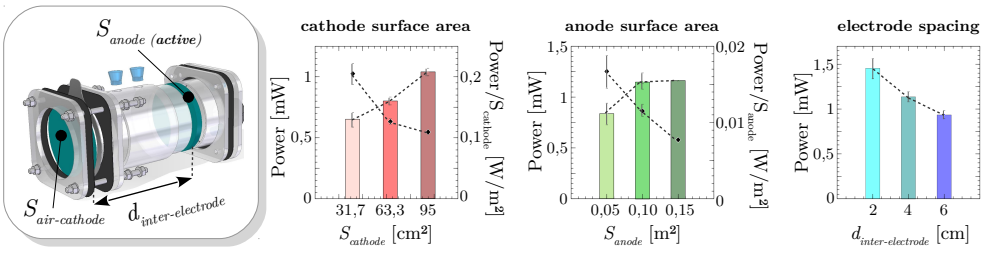

***Corresponding author:**
Justine PAPILLON
Tel: +33 4 72 43 63 81
E-mail address : justine.papillon@insa-lyon.fr
Laboratoire MATEIS
25, avenue Jean Capelle
Bâtiment Saint Exupéry
69 621 Villeurbanne Cedex
FRANCE

1 Introduction

MFCs convert a part of the energy contained in biodegradable substrates directly into electricity through the formation of an electroactive biofilm on the surface of their anode [Du et al., 2007].

These bioelectrochemical systems, which have been subject to a lot of research over the last twenty years, still have very limited performance [Logan, 2009] (of the order of a few $W.m^{-2}$ at best [Oliot et al., 2017b]) which does not entitle them to compete with other renewable energy sources such as photovoltaic or conventional fuel cells [Rinaldi et al., 2008].

The use of MFCs is unlikely to be viable for massive electricity production but should not be completely neglected since it could be a perfect solution for energy harvesting. They could, for example, be used to power the more and more numerous wireless sensors whose current batteries need to be regularly replaced and can be a source of pollution for their surrounding environment [Thomas et al., 2013, Degrenne, 2012, Khaled, 2016]. Although not of primary interest in the present paper, note also that these MFCs come with other benefits such as treatment and recovery.

If we consider the use of MFCs in this perspective, in order to finally be used beyond the laboratory scale, it is vital today to develop systems that present the best compromise between energy efficiency / simplicity / cost / durability / scaling-up [Asensio et al., 2017, Logan et al., 2007, Kim et al., 2015, Paitier, 2017]. A few studies have already looked into this issue, developing full-scale pilots that operate on a long-term basis [Ieropoulos et al., 2016, Liang et al., 2018, Walter et al., 2020, Gajda et al., 2020, Lu et al., 2017]

One of the key points to achieve this is the development of new anode

materials. In this study, we have focused on the development of stainless steel anodes. With an excellent price/electrical resistivity ratio as well as excellent mechanical properties, easy forming and good stability over time, this material is not to be neglected in the field of MFCs [Sonawane et al., 2018]. Currently, only a few studies have examined stainless steel, but they have reported very promising results. The first study reporting the use of stainless steel as an anode material is that of Dumas [Dumas et al., 2008]. It shows that this type of anode has a complex behaviour which is partially controlled by the electrochemical and semiconductor properties of the oxide layer that forms on its surface. These conclusions were confirmed by Érable who showed the competitiveness of stainless steel bio-anodes under controlled electrochemical conditions, with current densities of 8.2 $A.m^{-2}$ [Erable and Bergel, 2009]. In 2012, Pocaznoi's work resulted in current densities of 20.6 $A.m^{-2}$ by polarising plane stainless steel anodes at -0.2 V *vs* SCE (Saturated Calomel Electrode) [Pocaznoi et al., 2012].

In this study we have investigated the influence of the cathode surface, $S_{cathode}$, and the anode surface, S_{anode}, on the electrical performance of single-chamber air-cathode MFCs in which the stainless steel anodes were implanted. To ensure that the new material developed in our study is integrated as well as possible within the reactors and allows to optimize the MFCs performances, it is absolutely necessary to design the $S_{cathode}/S_{anode}$ ratio. The objective was to maximise energy production while minimising the quantity of material used in order to minimise costs.

We have also studied the influence of the inter-electrode distance on energy production, which is another important factor [Liu et al., 2005, Cheng et al., 2006] .

Moreover, all the experiments were carried out by supplying the MFCs with activated sludge (in real operating conditions) then a synthetic medium (in an optimized environment) in order to observe the effect of the type of electrolyte used on the observed trends.

2 Experimental

2.1 MFC construction

Single-chamber MFCs with an electrolyte volume of 850 mL and a cross sectional area, $S_{reactor}$, equal to 104 cm^2 were used for all of the experiments

performed in this study.

These reactors were equipped with manually fabricated air-cathodes according to the protocol defined by Middaugh [Middaugh et al., 2009]. These cathodes had, on their inner surface in direct contact with the electrolyte, a layer of platinum (0.5 mg.L^{-1}) which was used as a catalyst. The electrical connection of this electrode to the external circuit was ensured by a stainless steel sheet on its periphery.

The anodes were made up of an entangled 304L stainless steel monofilament with a diameter of 280 µm. These materials were initially developped for mechanical and vibration damping applications [Courtois et al., 2012]. Their electrical connection was established through the end of the monofilament which is connected outside of the reactor.

The projected surface area of cathode and anode was simply determined by the formula:

$$S_{projected} = \pi \times \left(\frac{\varnothing_{electrode}}{2} \right)^2 \tag{1}$$

with $\varnothing_{electrode}$ the diameter of the cathode or the anode.

For cathodes, the projected surface area was equivalent to the developed surface area. Nevertheless, for anodes, which are made of architectural materials, these two parameters were not equivalent. The developed anode surface, also called active surface, was determined by geometrical considerations:

$$S_{developed} = 2\pi \times \left(\frac{\varnothing_{monofilament}}{2} \right) \times L_{monofilament} \tag{2}$$

with $\varnothing_{monofilament}$ and $L_{monofilament}$, the diameter and length of the monofilament composing it, measured by the operator.

The volume fraction of monofilament within the anode, *Vf*, was also a parameter easy to determine:

$$Vf = \left(\frac{V_{monofilament}}{V_{global}} \right) = \left(\frac{L_{monofilament} \times \varnothing^2_{monofilament}}{h_{anode} \times \varnothing^2_{anode}} \right) \tag{3}$$

with h_{anode} and $\varnothing_{anode}$, the thickness and the diameter of the anode.

The design of these MFCs made it possible to easily modify various parameters to study their influence on electrical performance. In this study, the influence of the parameters described in the following paragraphs could thus be studied.

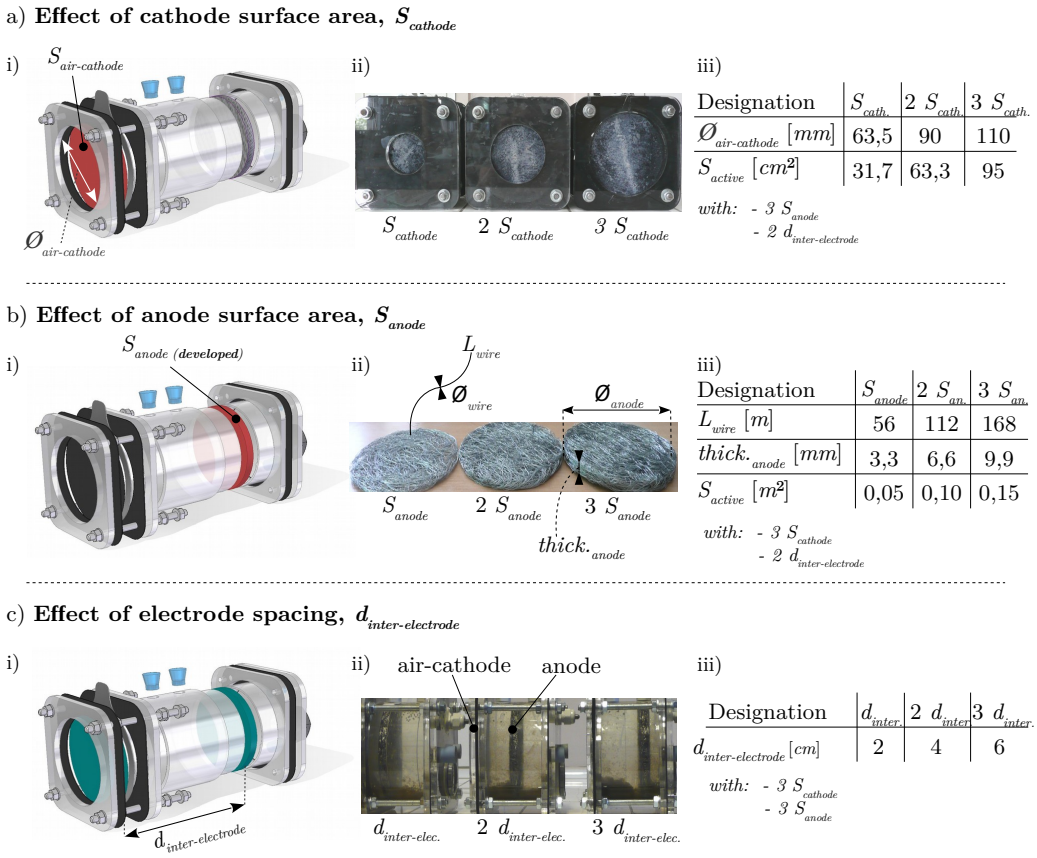

Figure 1: Experimental set-up to measure the influence of: a) cathode surface area, b) anode surface area and c) electrode spacing. i) schematic view of the reactors used; ii) photographs of the parameters tested; iii) dimensions of the parameters tested;

2.1.1 Cathode surface area

In order to quantify the influence of the cathode surface, the mounting plate that holds the air-cathodes in position could be modified. The diameter of the cathode in contact with the ambient air and the electrolyte could thus be changed in order to modulate the active cathode surface.

Figure 1 a) summarizes the dimensions of the air-cathodes tested during this campaign.

In order to demonstrate the effect of the cathode surface alone, the other parameters were identical for all reactors, with anodes (stainless steel, *Ø wire* = 280 µm, volume fraction $Vf = 10$ %, projected surface $S_{projected} = 104$ cm^2 and $S_{active} = 0.15$ m^2) and electrode spacing (4 cm) similar regardless of the cathodes used.

2.1.2 Anode surface area

The novel 3D anodes developed in this study, in addition to being simple and inexpensive, were very easily adaptable.

By modifying the length of the monofilaments used, anodes with different active surfaces were manufactured. The diameters of the anodes, however, remained the same, so the projected surfaces were the same for all anodes (104 cm^2). In order to keep the volume fractions of monofilament constant, the thickness of the anodes has been modified so that V_f was always equal to 10 %.

The characteristic dimensions of the tested anodes are summarized in Figure 1 b).

For all MFCs with different anode surfaces tested, the cathode surface was 95 cm^2 and the inter-electrode distance was 4 cm.

2.1.3 Electrode spacing

The reactors used were equipped with spacers inside the main tube which allow us to easily modify the spacing between the two electrodes. Tests were thus performed with inter-electrode distances of 2, 4 and 6 cm.

Figure 1 c) summarizes the dimensions of the MFCs tested during this campaign.

The air-cathodes ($S_{projected} = 95$ cm^2) and the anodes used (stainless steel, *Ø wire* = 280 µm, $Vf = 10$ %, $S_{projected} = 104$ cm^2 and $S_{active} = 0.15$ m^2) during these tests were all identical.

2.2 MFC operation

MFCs were inoculated with batches of activated sludge collected in the experimental hall of the IRSTEA (Institut National de la Recherche en Sciences et Technologies pour l'Environnement et l'Agriculture) on the site of the Feyssine wastewater treatment plant (69100 Villeurbanne - FRANCE).

After approximately 10 days of inoculation, MFCs were fed with batches of synthetic medium (mineral solution composed of a phosphate buffer (1,984 mM of KH_2PO_4, 3,127 mM of $Na_2HPO_4.12H_2O$) as well as mineral salts (9,908 mM of NH_4Cl, 0,510 mM of $CaCl_2.2H_2O$, 0,492 mM of $MgCl_2$. $6H_2O$) and a trace element solution (containing 0,081 mM H_3BO_3, 0,037 mM $ZnCl_2$, 0,022 mM $CuCl_2$ and 0,420 mM $CoCl_2$, $6H_2O$)) doped with acetate, CH_3COO^-, (16,937 mM, i.e. 1 $g.L^{-1}$) which acted as substrate.

MFCs were operated in parallel, at room temperature and in the dark to prevent algae growth. The ionic conductivity of the synthetic medium was about 3.2 $mS.cm^{-1}$ and the pH was 7.2.

The three parameters tested in this study (cathode surface, anode surface and electrode spacing) were the subject of completely independent test campaigns. For each test campaign, only one parameter varied, the others remained constant, in order to easily identify its effect on electrical performance.

For each parameter tested, the reactors were systematically doubled or tripled in order to take into account the large dispersion sometimes observed, characteristic of biological systems, and it was verified that the results were reproducible over at least three cycles.

2.3 Analyses

The voltage at the terminals of the MFC, E, was measured using a variable external resistor. The current delivered by the cell, I, was determined by Ohm's law:

$$I = E/R_{ext} \tag{4}$$

where R_{ext} is the external resistance applied to the terminals of the MFC and the power delivered by the MFC was determined by the formula:

$$P = E \times I \tag{5}$$

An R_{ext} of 1 kΩ was imposed on the cell terminals [Zhang et al., 2011] and the evolution of the voltage between the anode and the cathode was recorded.

Power ($P = \mathrm{f}(I)$) and polarization ($E = \mathrm{f}(I)$) curves were recorded daily during ~ 30 days. This was done by gradually varying the external resistance imposed from open circuit conditions ($R_{ext} = \infty$) to short circuit conditions ($R_{ext} = 0\ \Omega$) with a sampling time interval of 3 minutes.

These tests allowed us to determine:

- OCV, the open circuit voltage;
- P_{max}, the maximum power;
- R_{int}, the internal resistance of the cell, determined using Jacobi's law:

$$R_{ext} = R_{int} \quad when \quad P = P_{max}. \tag{6}$$

During these campaigns aiming at measuring the influence of electrode surfaces, the power and current values were normalized by the electrode surfaces in order to compare the results more easily.

3 Results and Discussion

3.1 Influence of $S_{cathode}$

The results of the polarization tests conducted on MFCs with different cathode surface areas are shown in Figure 2 and the parameters of the curves are summarized in Table 1.

Parameters tested	**Electrolyte type**	**Designation**	**Value** [cm^2]	OCV [mV]	P_{max} [µW]	$P_{max}/S_{reactor}$ [$mW.m^{-2}$]	$P_{max}/S_{cathode}$ [$mW.m^{-2}$]	R_{int} [Ω]
Cathode surface area	activated sludge	$S_{cathode}$	31.7	703 *(± 2)*	332 *(± 0.7)*	31.9 *(± 0.1)*	105 *(± 0.2)*	245 *(± 5)*
		2 $S_{cathode}$	63.3	697 *(± 9)*	499 *(± 4)*	48.0 *(± 0.4)*	79 *(± 0.6)*	177 *(± 0.9)*
		3 $S_{cathode}$	95	718 *(± 8)*	720 *(± 59)*	69.2 *(± 5.7)*	76 *(± 6)*	135 *(± 6)*
	synthetic medium	$S_{cathode}$	31.7	714 *(± 7)*	650 *(± 55)*	62.5 *(± 5.3)*	204 *(± 18)*	127 *(± 12)*
		2 $S_{cathode}$	63.3	723 *(± 0.9)*	801 *(± 32)*	77.0 *(± 3.1)*	127 *(± 5)*	111 *(± 0.3)*
		3 $S_{cathode}$	95	756 *(± 7)*	1039 *(± 31)*	99.9 *(± 3)*	109 *(± 3)*	90 *(± 0.6)*

Table 1: Performances of MFC with different cathode surface areas.

Performances of MFCs are significantly influenced by the cathode surface which seems to be, in the configuration retained in this study, the limiting electrode.

Polarization tests show that increasing $S_{cathode}$ leads to an increase in OCV. This phenomenon has already been mentioned in the literature and explained by an increase of the cathode potential (for a constant anode potential) [Cheng and Logan, 2011].

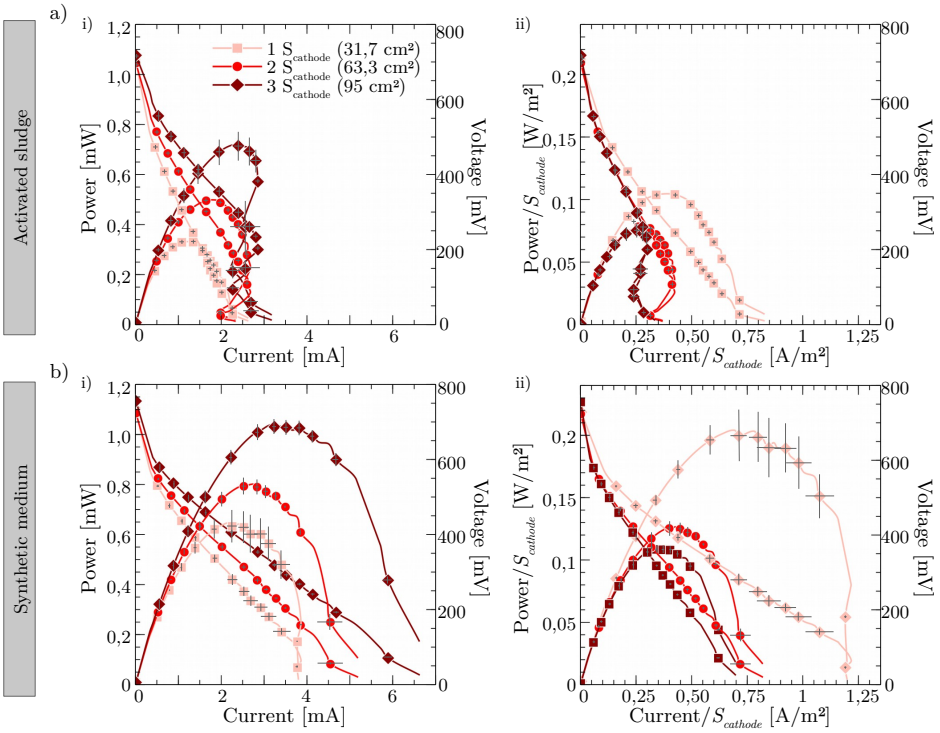

Figure 2: Influence of cathode surface area. Performances of MFC fed with: a) activated sludge and b) synthetic medium. i) polarization and power curves and ii) same curves normalized.

Similarly, the larger the cathode surface area, the higher P_{max}. The increase in P_{max} is a direct consequence of the decrease in R_{int}. In a more detailed study [Houghton et al., 2016] it has been shown that an increase in $S_{cathode}$ effectively leads to a decrease in $R_{cathode}$ and an increase in electrode capacitance .

In this study, with activated sludge, doubling the cathode surface area from $S_{cathode}$ to 2 $S_{cathode}$ allows a gain in P_{max} of +50.3 % and further increasing the surface area from 2 $S_{cathode}$ to 3 $S_{cathode}$ allows a further gain of +44.3 %. The same trends are confirmed with the synthetic medium, with an increase in P_{max} of +23.3 % between $S_{cathode}$ and 2 $S_{cathode}$ and +29.6 % between 2 $S_{cathode}$ and 3 $S_{cathode}$. However, the influence of the cathode surface seems more limited with the synthetic medium. These conclusions

contrast with those of Cheng who observed a greater influence of $S_{cathode}$ when MFCs are fed with synthetic medium with higher conductivity and substrate concentration [Cheng and Logan, 2011]. This discrepancy may be related to an underestimation of MFCs performance due to the progressive (bio)fouling of the internal surface of air-cathodes. Oliot has recently shown that this phenomenon indeed occurs very quickly after the beginning of the tests and is not easy to detect given the apparent stability of the results caused by the concomitant improvement of the bioanode performance [Oliot et al., 2016]. In our study, we tried to limit the deleterious effect of this fouling, induced by the formation of a biofilm mixed with the precipitation of mineral salts, by scraping the surface of the cathode. This had no effect on performance. Only the replacement of the cathode by a new one allowed to completely restore the initial performance of the cell. For this reason, a new cathode was used for each test campaign.

After normalization of current and power by the cathode surface area, it appears that MFCs with the smallest cathode surface area, $S_{cathode}$, are the most efficient. Nevertheless, it is also of interest to point out that the normalized power values are similar for 2 $S_{cathode}$ and 3 $S_{cathode}$. A quasi-linear relationship is observed between P_{max} and $S_{cathode}$. Since the smaller cathodes have higher $P_{max}/S_{cathode}$ values, it suggests that other parameters are certainly involved in the performances of MFCs [Chung et al., 2011].

3.2 Influence of S_{anode}

Figure 3 shows polarization curves obtained with MFCs with different developed anode surface areas, S_{anode}. Table 2 summarizes the parameters extracted from these curves.

Influence of anode surface area on OCV appears to be little for MFCs fed with activated sludge and even almost insignificant for those fed with synthetic medium. These results contradict those of Lanas, who found a slight increase in OCV when S_{anode} increased, related to a decrease in electrode potential [Lanas et al., 2014].

P_{max} increases by +17.6 % when the anode surface area is doubled, from S_{anode} to 2 S_{anode}, then only by +8.7 % from 2 S_{anode} to 3 S_{anode} with MFC fed with activated sludge. With synthetic medium, there is an increase in P_{max} of +37.8 % between S_{anode} and 2 S_{anode} compared to only +1.0 % between 2 S_{anode} and 3 S_{anode}. These results are to parallel moreover with the small decrease of the internal resistance of the cells when the anode surface area

increases.

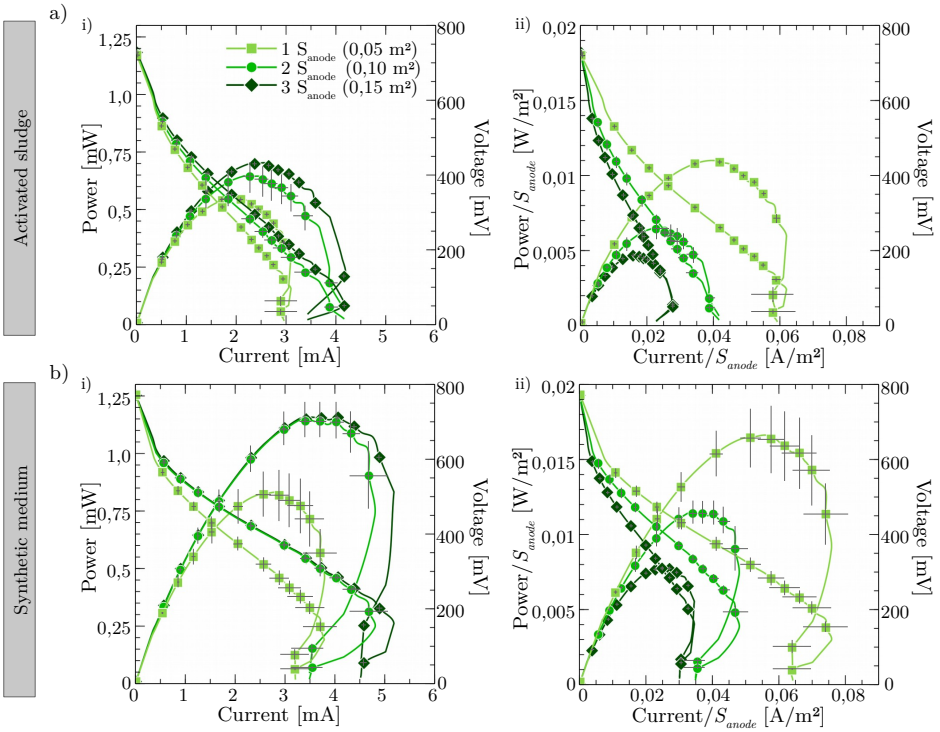

Figure 3: Influence of anode surface area. Performances of MFC fed with: a) activated sludge and b) synthetic medium. i) polarization and power curves and ii) same curves normalized.

Parameters tested	**Electrolyte type**	**Designation**	**Value** [m^2]	OCV [mV]	P_{max} [µW]	$P_{max}/S_{reactor}$ [mW.m^{-2}]	P_{max}/S_{anode} [mW.m^{-2}]	R_{int} [Ω]
Anode surface area	activated sludge	S_{anode}	0.05	720 *(± 3)*	550 *(± 5)*	52.9 *(± 0.5)*	11.0 *(± 0.1)*	148 *(± 1)*
		2 S_{anode}	0.10	724 *(± 4)*	647 *(± 55)*	62.2 *(± 5.3)*	6.5 *(± 0.5)*	127 *(± 6)*
		3 S_{anode}	0.15	728 *(± 0.1)*	703 *(± 10)*	67.6 *(± 1)*	4.7 *(± 0.1)*	117 *(± 1)*
	synthetic medium	S_{anode}	0.05	772 *(± 2)*	833 *(± 107)*	80.1 *(± 10.3)*	16.7 *(± 2.0)*	114 *(± 12)*
		2 S_{anode}	0.10	768 *(± 6)*	1148 *(± 66)*	110.4 *(± 6.3)*	11.5 *(± 0.7)*	85 *(± 2)*
		3 S_{anode}	0.15	771 *(± 1)*	1161 *(± 3)*	111.6 *(± 0.3)*	7.7 *(± 0.1)*	86 *(± 0.5)*

Table 2: Performances of MFC with different anode surface areas.

Anodes with the smallest surface area, S_{anode}, seem to limit the performance of MFCs since increasing the anode surface area will generate more

power. Nevertheless, using an anode surface area greater than 2 S_{anode}, the increase of S_{anode} seems to have a very limited impact on the electrical performance of the MFC, particularly when the cell is powered with a synthetic medium. The anode no longer appears to be a limiting factor. These observations corroborate the conclusion drawn in paragraph 3.1, where the anode surface used was 3 S_{anode} and the cathode was indeed the limiting electrode.

Normalized by the developed anode surface area, anodes with the smallest surface areas are the most efficient.

The often non-limiting nature of the anode surface has already been shown in many studies [Hutchinson et al., 2011, Liu et al., 2008, Logan et al., 2007, Lanas and Logan, 2013, Kim et al., 2015, Uría et al., 2012]. However, it is essential for each new electrode material developed to check which electrode is limiting in the retained cell configuration. In our study, it will thus be possible to optimize the quantity of material useful for the manufacturing of the anodes, which can be interesting from an economic point of view for real applications of MFCs.

In the case of our research, in addition to the tests presented in this article, which have a duration of 30 days, we have carried out long-term tests. After 130 days of continuous testing, we found no trace of corrosion on the stainless steel anode and no loss of electrode mass. Imposing a low potential on the anode which remains away from the pitting potential of the stainless steel is certainly helping. At the same time, these long-term tests also made it possible to show that the 3D structure of the anodes we are developing makes it possible to limit clogging, which is a major problem in the field of porous electrodes.

3.3 Influence of $d_{inter-electrode}$

Polarization curves obtained during the campaign to identify the influence of electrode spacing are shown in Figure 4. Table 3 summarizes the parameters extracted from these curves.

Regardless of the type of electrolyte used, activated sludge or synthetic medium, similar conclusions can be drawn from the polarisation tests: a decrease of electrode spacing leads to a decrease of R_{int} resulting in an increase of P_{max}. Decreasing the distance between the electrodes reduces the ion transport distance and thus decreases the ohmic resistance of the cell.

In the literature, the electrode spacing effect has been reported in a few studies. Liu, for example, has reported the increase in P_{max} from 720 to

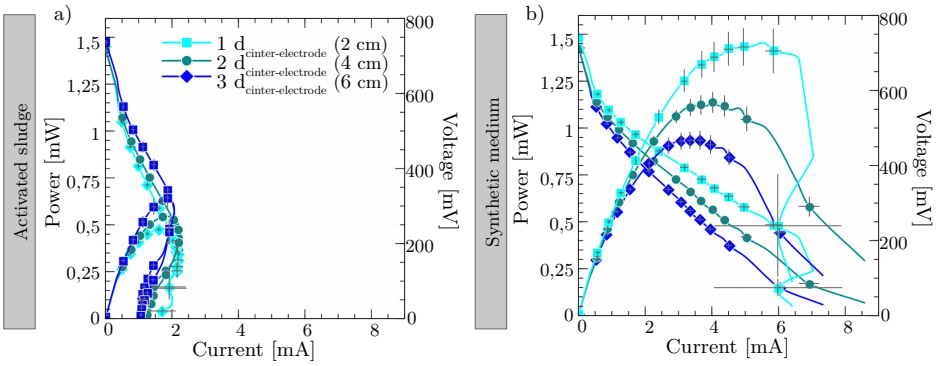

Figure 4: Influence of electrode spacing. Performances of MFC fed with: a) activated sludge and b) synthetic medium.

Parameters tested	**Electrolyte type**	**Designation**	**Value** [cm]	*OCV* [mV]	P_{max} [µW]	$P_{max}/S_{reactor}$ [mW.m^{-2}]	R_{int} [Ω]
Electrode spacing	activated sludge	$d_{inter-elec.}$	2	737 *(± 6)*	641 *(± 51)*	61.6 *(± 4.9)*	160 *(± 8)*
		2 $d_{inter-elec.}$	4	719 *(± 4)*	545 *(± 7)*	52.4 *(± 0.7)*	177 *(± 1)*
		3 $d_{inter-elec.}$	6	725 *(± 4)*	473 *(± 10)*	45.5 *(± 1)*	202 *(± 6)*
	synthetic medium	$d_{inter-elec.}$	2	739 *(± 4)*	1454 *(± 111)*	139.8 *(± 10.7)*	63 *(± 4)*
		2 $d_{inter-elec.}$	4	710 *(± 1)*	1136 *(± 56)*	109.2 *(± 5.4)*	77 *(± 3)*
		3 $d_{inter-elec.}$	6	713 *(± 39)*	937 *(± 46)*	90.1 *(± 4.4)*	88 *(± 2)*

Table 3: Performances of MFC with different electrode spacing.

1210 mW.m^{-2} when the electrode spacing is decreased from 4 cm to 2 cm [Liu et al., 2005]. He has also shown that these results correlate with a decrease in R_{int} from 161 to 77 Ω for 4 and 2 cm respectively.

Cheng completed these results by decreasing the electrode spacing to a value of 1 cm. In this case, P_{max} decreases from 811 mW.m^{-2} for a distance of 2 cm to only 423 mW.m^{-2} for 1 cm [Cheng et al., 2006]. R_{int}, however, decreases from 35 Ω to 16 Ω for 2 and 1 cm. These results show an optimum of inter-electrodes distance. When the electrodes are very close to each other, there is a risk that the oxygen that passes through the cathode-air diffuses to the anode and hinders the anodic bacterial activity. A decrease in the voltage at the terminals of the MFC is then observed (820 mV for 2 cm against 797 mV for 1 cm) and is induced essentially by an increase in the negative potential of the anode (552 mV for 2 cm against 531 mV for 1 cm).

The low ionic conductivity of MFCs imposed by the use of micro-organisms drastically limits their performance. One of the solutions commonly used to reduce the internal resistance of the reactors is to bring the two electrodes closer together. Nevertheless, an optimum should be determined so that the activity of the anodic biofilm is not limited by the diffusion of oxygen on the surface of the electrode. Some studies then add separators between the anode and the cathode [Fan et al., 2007, Oliot et al., 2017a, Moon et al., 2015, Ahn and Logan, 2013]. This limits the diffusion of oxygen at the anode and therefore the distance between electrodes is smaller, but, in return, separators limit the ion transport within the cell and can become clogged, which increases the internal resistance of the cell and decreases its electrical performances.

In the case of the present study, the 2 cm electrode spacing was chosen as the most efficient because it seems that these effects of reduced performance due to the diffusion of oxygen to the anode are not yet observed.

The effect of the electrode spacing also appears to be exacerbated by the conductivity of the electrolyte, as when the MFCs are fed with activated sludge, reducing the electrode spacing from 6 to 4 cm results in a gain of +15 % of P_{max} and 6 to 2 cm of +35.5 %, whereas when they are fed with synthetic medium, which has a higher conductivity, reducing the electrode spacing from 6 to 4 cm results in a gain of +21.3 % of P_{max} and 6 to 2 cm of +55.2 %. These results corroborate those of Jang who showed that when the internal resistance of a MFC is high (for example, due to a higher ohmic resistance of the cell caused by a lower electrolyte conductivity), the influence of the inter-electrode distance is much less important [Jang et al., 2004]. His work showed a decrease in P_{max} of 1.3 mW.m^{-2} for a spacing of 10 cm to 1.25 mW.m^{-2} for 30 cm with high R_{int} values of 668 Ω and 690 Ω and OCV values of about 520 mV and about 480 mV respectively.

4 Conclusion

This study focuses on the architecture optimization of MFCs with innovative stainless steel entanglements anodes. Figure 5 summarizes results achieved. Increasing the cathode surface improves performance while rapidly a saturation of performance can be observed when anode surface is increased. An optimal electrode spacing of 2 cm is observed. Optimising the quantity of materials used in order to limit costs is a crucial issue in the development

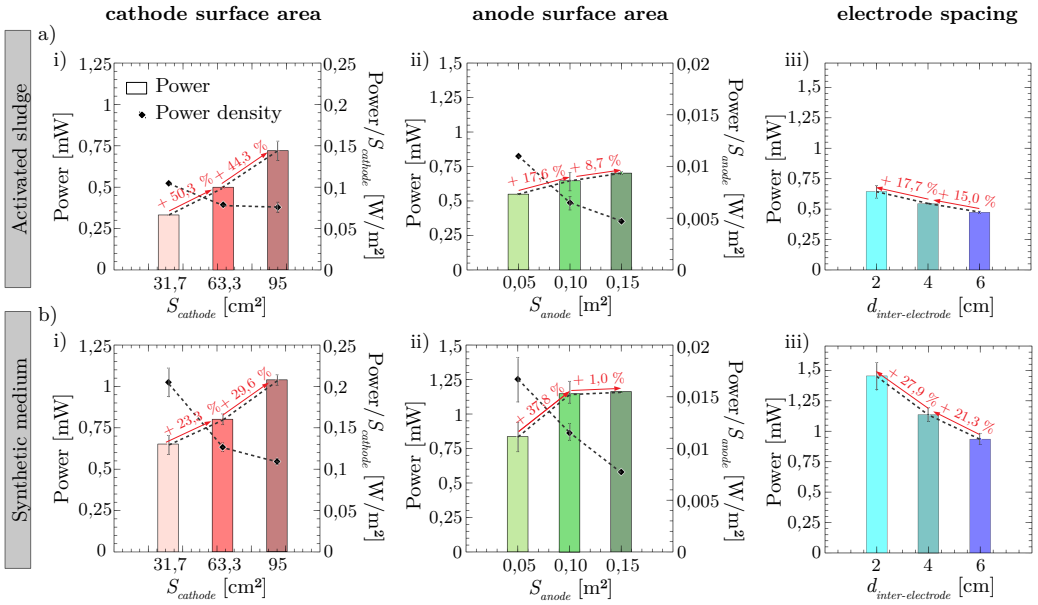

Figure 5: Maximum power obtained with different: i) cathode surface area, ii) anode surface area and iii) electrode spacing for MFCs fed with: a) activated sludge and b) synthetic medium. Histograms represent power values obtained, in mW, and points power values normalized by the cathode or anode surface, in W.m^{-2}.

of MFCs for efficient energy-harvesting solutions. As small reactors provide better performance, it is absolutely essential to develop stacked MFCs more efficient than large MFCs.

5 Data availability

The raw/processed data required to reproduce these findings cannot be shared at this time because of technical or time limitations.

Acknowledgements

This study was supported by Auvergne-Rhône-Alpes Region (ARC Énergies).

References

[Ahn and Logan, 2013] Ahn, Y. and Logan, B. (2013). Altering anode thickness to improve power production in microbial fuel cells with different electrode distances. *Energy & Fuels*, 27:271–276.

[Asensio et al., 2017] Asensio, Y., Montes, I., Fernandez-Marchante, C., Lobato, J., Cañizares, P., and Rodrigo, M. (2017). Selection of cheap electrodes for two-compartment microbial fuel cells. *Journal of Electroanalytical Chemistry*, 785:235–240.

[Cheng et al., 2006] Cheng, S., Liu, H., and Logan, B. E. (2006). Increased power generation in a continuous flow MFC with advective flow through the porous anode and reduced electrode spacing. *Environmental Science and Technology*, 40:2426–2432.

[Cheng and Logan, 2011] Cheng, S. and Logan, B. E. (2011). Increasing power generation for scaling up single-chamber air cathode microbial fuel cells. *Bioresource Technology*, 102:4468–4473.

[Chung et al., 2011] Chung, K., Fujiki, I., and Okabe, S. (2011). Effect of formation of biofilms and chemical scale on the cathode electrode on the performance of a continuous two-chamber microbial fuel cell. *Bioresource Technology*, 102:355–360.

[Courtois et al., 2012] Courtois, L., Maire, E., Perez, M., Rodney, D., Bouaziz, O., and Brechet, Y. (2012). Mechanical properties of monofilament entangled materials. *Advanced Engineering Materials*.

[Degrenne, 2012] Degrenne, N. (2012). *Gestion de l'énergie despiles à combustible microbiennes*. PhD thesis.

[Du et al., 2007] Du, Z., Li, H., and Gu, T. (2007). A state of the art review on microbial fuel cells: A promising technology for wastewater treatment and bioenergy. *Biotechnology Advances*, 25:464–482.

[Dumas et al., 2008] Dumas, C., Mollica, A., Féron, D., Basseguy, R., Etcheverry, L., and Bergel, A. (2008). Checking graphite and stainless anodes with an experimental model of marine microbial fuel cell. *Bioresource Technology*, 99:8887–8894.

[Erable and Bergel, 2009] Erable, B. and Bergel, A. (2009). First air-tolerant effective stainless steel microbial anode obtained from a natural marine biofilm. *Bioresource Technology*, 100:3302–3307.

[Fan et al., 2007] Fan, Y., Hu, H., and Liu, H. (2007). Enhanced Coulombic efficiency and power density of air-cathode microbial fuel cells with an improved cell configuration. *Journal of Power Sources*, 171(2):348–354.

[Gajda et al., 2020] Gajda, I., Obata, O., Salar-garcia, M. J., Greenman, J., and Ieropoulos, I. A. (2020). Bioelectrochemistry Long-term bio-power of ceramic microbial fuel cells in individual and stacked configurations. *Bioelectrochemistry*, 133.

[Houghton et al., 2016] Houghton, J., Santoro, C., Soavi, F., Serov, A., Ieropoulos, I., Arbizzani, C., and Atanassov, P. (2016). Supercapacitive microbial fuel cell: Characterization and analysis for improved charge storage/delivery performance. *Bioresource Technology*, 218:552–560.

[Hutchinson et al., 2011] Hutchinson, A. J., Tokash, J. C., and Logan, B. E. (2011). Analysis of carbon fiber brush loading in anodes on startup and performance of microbial fuel cells. *Journal of Power Sources*, 196(22):9213–9219.

[Ieropoulos et al., 2016] Ieropoulos, I. A., Stinchcombe, A., Gajda, I., Forbes, S., Merino-Jimenez, I., Pasternak, G., and Sanchez-Herranza, D. Greenman, J. (2016). Pee power urinal – microbial fuel cell technology field trials in the context of sanitation. *Environmental Science: Water Research & Technology*, (2):336–343.

[Jang et al., 2004] Jang, J. K., Pham, T. H., Chang, I. S., Kang, K. H., Moon, H., Cho, K. S., and Kim, B. H. (2004). Construction and operation of a novel mediator- and membrane-less microbial fuel cell. *Process Biochemistry*, 39(8):1007–1012.

[Khaled, 2016] Khaled, F. (2016). *Contribution à la Valorisation Electrique des Piles à Combustible Microbiennes*. PhD thesis.

[Kim et al., 2015] Kim, K.-Y., Yang, W., and Logan, B. E. (2015). Impact of electrode configurations on retention time and domestic wastewater treatment efficiency using microbial fuel cells. *Water Research*, 80:41–46.

[Lanas et al., 2014] Lanas, V., Ahn, Y., and Logan, B. (2014). Effects of carbon brush anode size and loading on microbial fuel cell performance in batch and continuous mode. *Journal of Power Sources*, 247:228–234.

[Lanas and Logan, 2013] Lanas, V. and Logan, B. E. (2013). Evaluation of multi-brush anode systems in microbial fuel cells. *Bioresource Technology*, 148:379–385.

[Liang et al., 2018] Liang, P., Duan, R., Jiang, Y., Zhang, X., Qiu, Y., and Huang, X. (2018). One-year operation of 1000-L modularized microbial fuel cell for municipal wastewater treatment. *Water Research*, 141:1–8.

[Liu et al., 2008] Liu, H., Cheng, S., Huang, L., and Logan, B. E. (2008). Scale-up of membrane-free single-chamber microbial fuel cells. *Journal of Power Sources*, 179:274–279.

[Liu et al., 2005] Liu, H., Cheng, S. A., and Logan, B. E. (2005). Power generation in fed-batch microbial fuel cells as a function of ionic strength, temperature, and reactor configuration. *Environmental Science & Technology*, 39(14):5488–5493.

[Logan, 2009] Logan, B. (2009). Exoelectrogenic bacteria that power microbial fuel cells. *Nature Reviews Microbiology*, 7(5):375–381.

[Logan et al., 2007] Logan, B., Cheng, S., Watson, V., and Estadt, G. (2007). Graphite fiber brush anodes for increased power production in air-cathode microbial fuel cells. *Environmental Science and Technology*, 41:3341–3346.

[Lu et al., 2017] Lu, M., Chen, S., Phadke, S., Salvacion, M., Mirhosseini, A., Chan, S., Carpenter, K., Cortese, R., and Bretschger, O. (2017). Long-term performance of a 20-L continuous fl ow microbial fuel cell for treatment of brewery wastewater. *Journal of Power Sources*, 356:274–287.

[Middaugh et al., 2009] Middaugh, J., Cheng, S., and Liu, W. (2009). How to Make Cathodes with a Diffusion Layer for Single-Chamber Microbial Fuel Cells.

[Moon et al., 2015] Moon, J. M., Kondaveeti, S., Lee, T. H., Song, Y. C., and Min, B. (2015). Minimum interspatial electrode spacing to optimize air-cathode microbial fuel cell operation with a membrane electrode assembly. *Bioelectrochemistry*, 106:263–267.

[Oliot et al., 2016] Oliot, M., Etcheverry, L., and Bergel, A. (2016). Removable air-cathode to overcome cathode biofouling in microbial fuel cells. *Bioresource Technology*, 221:691–696.

[Oliot et al., 2017a] Oliot, M., Etcheverry, L., Mosdale, A., Basseguy, R., Délia, M.-L., and Bergel, A. (2017a). Separator electrode assembly (SEA) with 3-dimensional bioanode and removable air-cathode boosts microbial fuel cell performance. *Journal of Power Sources*, 356:389–399.

[Oliot et al., 2017b] Oliot, M., Etcheverry, L., Mosdale, R., and Bergel, A. (2017b). Microbial fuel cells connected in series in a common electrolyte underperform: Understanding why and in what context such a set-up can be applied. *Electrochimica Acta*, 246:879–889.

[Paitier, 2017] Paitier, A. (2017). *Etude de la mise à l'échelle des Piles à Combustible Microbiennes : collecteurs de courant et hydrodynamique*. PhD thesis.

[Pocaznoi et al., 2012] Pocaznoi, D., Calmet, A., Etcheverry, L., Erable, B., and Bergel, A. (2012). Stainless steel is a promising electrode material for anodes of microbial fuel cells. *Energy and Environmental Science*, 5(11):9645–9652.

[Rinaldi et al., 2008] Rinaldi, A., Mecheri, B., Garavaglia, V., Licoccia, S., Di Nardo, P., and Traversa, E. (2008). Engineering materials and biology to boost performance of microbial fuel cells: a critical review. *Energy & Environmental Science*, 1:417–429.

[Sonawane et al., 2018] Sonawane, J., Patil, S., Ghosh, P., and Adeloju, S. (2018). Low-cost stainless-steel wool anodes modified with polyaniline and polypyrrole for high-performance microbial fuel cells. *Journal of Power Sources*, 379:103–114.

[Thomas et al., 2013] Thomas, Y., Picot, M., Carer, A., Berder, O., Sentieys, O., and Barrière, F. (2013). A single sediment-microbial fuel cell powering a wireless telecommunication system. *Journal of Power Sources*, 241:703–708.

[Uría et al., 2012] Uría, N., Sánchez, D., Mas, R., Sánchez, O., Muñoz, F. X., and Mas, J. (2012). Effect of the cathode/anode ratio and the choice

of cathode catalyst on the performance of microbial fuel cell transducers for the determination of microbial activity. *Sensors and Actuators, B: Chemical*, 170:88– 94.

[Walter et al., 2020] Walter, X. A., You, J., Win, J., Bajarunas, U., Greenman, J., and Ieropoulos, I. A. (2020). From the lab to the fi eld : Self-stratifying microbial fuel cells stacks directly powering lights. *Applied Energy*, 277(July).

[Zhang et al., 2011] Zhang, L., Zhu, X., Li, J., Liao, Q., and Ye, D. (2011). Biofilm formation and electricity generation of a microbial fuel cell started up under different external resistances. *Journal of Power Sources*, 196(15):6029–6035.